

**Introduction:** Craters are ubiquitous across most solid surfaces in the solar system and are useful for a wide variety of applications. In 2012, we released the largest global crater database of Mars, containing over 380,000 craters [1,2] (Fig. 1), and we estimate that it is a complete sampling of craters with diameters  $D \geq 1$  km (*i.e.*, while there are likely some missed craters, any missing  $\geq 1$  km should not change the population statistics). This database contains many morphologic and morphometric features of included craters. We have also been working to classify the craters as secondary or primary, such that a true primary crater population of the planet can be used for future research. This abstract details some of the database creation process, secondary classification, and how one can obtain the database and submit corrections.

**Construction of the Crater Database:** All craters were identified manually in THEMIS Day IR mosaics ( $\gg 99\%$  coverage [3]), Viking MDIM 2.1 where gaps exist in THEMIS coverage, CTX mosaics in isolated cases, and MOLA data. With a THEMIS resolution of  $\sim 100$  m/pix, we used *ArcGIS* software to outline each crater rim and cohesive ejecta blanket (if present) at  $\sim 500$  m vertex spacing. *Igor Pro* software is used to calculate best-fit circle and ellipse parameters for each crater. Each  $D \geq 3$  km crater was re-identified if possible in MOLA  $1/128^\circ$  gridded and point data to determine rim height, surface elevation, and floor depth, though recent work [4] shows the MOLA data introduce a shallowing bias for craters  $D < 10$  km. THEMIS data were used to visually classify crater interior and ejecta morphology, ejecta morphometry, and crater preservation state.

Our crater database includes MOLA- and THEMIS-based latitude, longitude, diameter, and ellipse parameters; MOLA-based rim, surrounding surface, and floor elevation; crater preservation state; three crater interior morphology descriptors and three ejecta morphologies; detailed morphometric data of cohesive ejecta; whether or not the crater is a likely secondary; the subjective likelihood the feature is a true impact crater; and official IAU name if it has one. Full details are available in [1,2] detailing how the database was constructed and basic trends and results in context with previous work.

**Secondary Crater Identification:** The database was overlaid on THEMIS Day IR global mosaics in *ArcMap* software, and the maps were searched multiple times for those craters that appear to be morphologically distinct secondary craters. Secondaries were craters identified by the following characteristics [5-8]:

- tightly clustered relative to surrounding craters,
- part of a herringbone ejecta pattern,
- entrained within a much larger crater's ejecta,

- and/or are highly elongated with one major axis end being shallower than the other end.

Fig. 1 shows the non-uniform contamination of secondary craters across Mars.

A caveat for this method is that it very likely under-estimates the true population of secondary craters because, by their nature, we cannot distinguish between primaries and "lone" secondaries that some argue form part of a global, background secondary crater population. We also cannot recognize if secondary craters start to dominate for crater diameters  $< 1$  km because the crater catalog is not complete for those craters globally (though is in some locations).

Another factor that contaminates our results are crater clusters formed by an impactor breaking up soon before impact because these can display morphologies very similar to secondary crater clusters [9]. While this is a contaminant, these crater clusters are themselves an additional contaminator of the primary crater population because, like secondaries, they form in a geologic instant and are tightly clustered spatially; they should be a spatially random contaminant, unlike secondaries. Ergo, their removal – or estimate of what crater would have formed from an intact primary – would also be necessary for applications of primary craters such as age-modeling.

**Analysis:** To determine a "global" value for the dominance of secondaries, two cumulative crater size-frequency distributions (SFDs) were calculated – one for primaries and one for secondaries. If the secondaries' SFD intersected and grew larger than the primaries' at any diameter, that would be considered the transition diameter. To calculate this on a regional basis, a 500, 1000, and 1500 km moving radius from every center of a  $1^\circ \times 1^\circ$  grid of the planet was taken and the craters within were analyzed in a similar manner, and they were also analyzed as a function of the latest global geologic maps [11].

**Results:** The global Mars results show that there is no intersection in the SFDs, so the population of secondaries did not dominate over primaries. They were approximately 20% of all  $D \geq 1$  km craters, however, indicating significant contamination. The secondary crater SFD slope shallows between 1 and 2 km relative to 2-10 km, indicating that the fraction of secondaries may be  $2\times$  our estimate which would raise the contamination to 33% of  $D \geq 1$  km craters.

Fig. 2 shows the results of performing this analysis over a  $1^\circ \times 1^\circ$  grid with a 500 km radius around each point. We performed the analysis for where secondaries match the primary population, where the onset diameter of secondary contamination is only 50% the abundance of primaries, and where it is 33% the abundance of primaries (alternatively: when 50%, 33%, and

25% of the craters per bin are secondaries). There are only four areas where the secondary crater population matches the primary crater population, and all are at  $D \leq 5$  km with most  $\leq 3$  km: the young, large Lomonosov and Lyot craters, north of Holden crater, and between Crise planum and Valles Marineris. When lowering the threshold to consider the population contaminated, the extent broadens as seen in the bottom panel of Fig. 2.

When extending the analysis to chronostratigraphic unit [11], we find no transition diameter on any terrain for  $D \geq 1$  km craters. For Noachian and Hesperian, the extrapolated transition is  $\sim 3/4$  km, and for Amazonian terrain it is  $\sim 1/2$  km. Smaller transition diameters are expected for younger terrain because it has not yet had a chance to accumulate large primaries that would generate km-scale secondaries. Noachian and Hesperian are similar because of the vast resurfacing that Mars experienced around the Noachian-Hesperian transition [e.g. 12,13]

**Status, Availability, and Community Corrections:** As of early 2014, the complete database contains  $\sim 632,000$  craters at diameters down to  $\sim 0.5$  km. Globally, the database is statistically complete to 0.96 km with estimated completeness locally to diameters as small as 0.76 km. We publicly released the approx. 385,000 craters only down to  $D = 1.0$  km; additional, smaller craters may be obtained by request. The  $\geq 1.0$  km crater catalog is available on the MRCTR / PIGWAD site operated by the USGS, in the Mars Crater Consortium section. It is also available on the website <http://craters.sjrdesign.net> that can be searched. That website also contains a feedback form where people can submit any potential problems / necessary fixes or changes. This database is not meant to be a static product, but one that is versioned, subject to additions (such as this secondary crater work not in the initial release) and corrections from community input; please contact the corresponding author for more information.

**References:** [1] Robbins & Hynek (2012a) doi: 10.1029/2011JE003966. [2] Robbins & Hynek (2012b) doi: 10.1029/2011JE003967. [3] Edwards *et al.* (2011) doi: 10.1029/2010JE003755. [4] Robbins & Hynek (2013) doi: 10.1016/j.pss.2013.06.019. [5] Shoemaker (1962). [6] Shoemaker (1965). [7] Oberbeck & Morrison (1974) doi: 10.1007/BF00562581. [8] Robbins & Hynek (2011) doi: 10.1029/2011JE003820. [9] Popova *et al.* (2007) doi: 10.1016/j.icarus.2007.02.022. [10] Robbins & Hynek (in rev.) *EPSL*. [11] Tanaka *et al.* (in press) USGS Map 3292. [12] Robbins *et al.* (2013) doi: 10.1016/j.icarus.2013.03.019. [13] Irwin *et al.* (2013) doi: 10.1002/jgre.20053. [14] Smith *et al.* (2001) doi: 10.1029/2000JE001364.

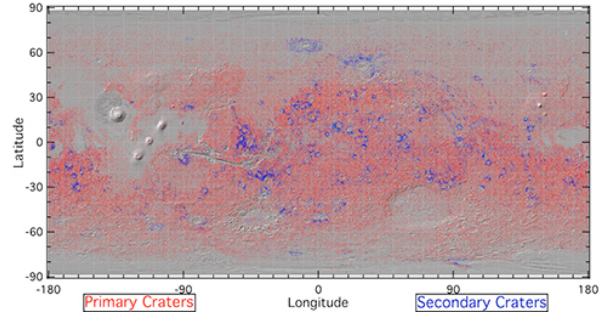


**Figure 1:** Mars shaded relief basemap [14] with craters with diameters  $\geq 1.0$  km from [1] overlotted as dots independent of crater size. Craters in red are those classified as primaries, craters in blue are those classified as secondaries.

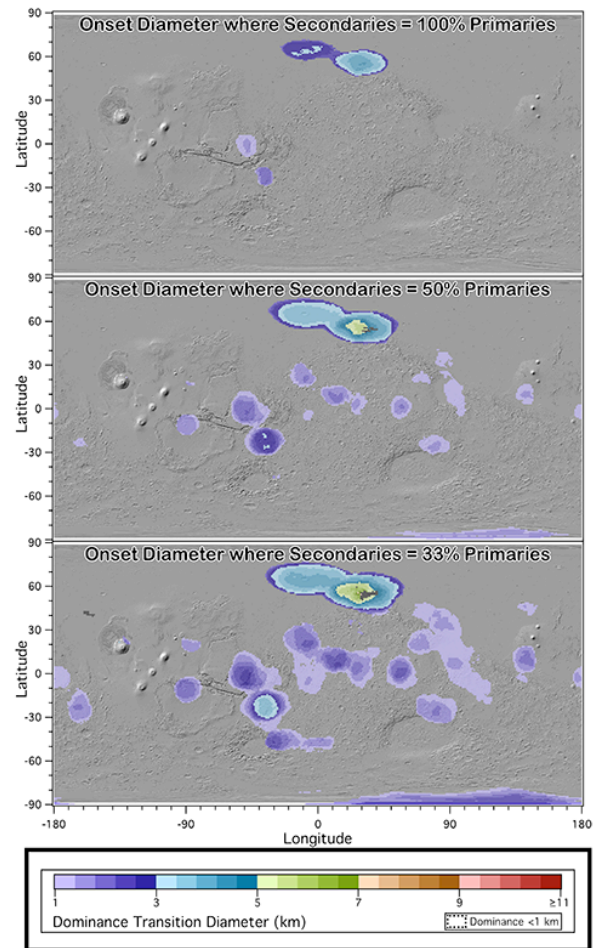


**Figure 2:** All craters in a radius 500 km from the center of each  $1^\circ \times 1^\circ$  bin were extracted from the final database and plotted as CSFDs. If there was a diameter at which the secondary crater CSFD became greater than the primary crater CSFD, that was saved as the bin value (top row). If it reached half as much as the primaries, that was middle row bin value, and one-third as much was the value for the bottom row. This transition diameter is color-coded per the legend at the bottom, and bins where the primary crater population dominated throughout were left as empty (transparent).